SLAC – PUB – 3398
August 1984
(T/E)

SEMIPHENOMENOLOGICAL SYNTHESIS OF MESON AND QUARK DYNAMICS AND THE E.M. STRUCTURE OF THE NUCLEON*

MANFRED GARI

Stanford Linear Accelerator Center
Stanford University, Stanford, California, 94305

and

Institut für Theoretische Physik,
Ruhr–Universität Bochum, W–Germany†

and

W. KRÜMPELMANN

Institut für Theoretische Physik,
Ruhr–Universität Bochum, W–Germany

Submitted to *Physical Review Letters*

* Work supported by the Department of Energy, contract DE – AC03 – 76SF00515
† *Permanent address*

ABSTRACT

We show that an extended vector dominance model which incorporates quark dynamics at large Q^2 via perturbative QCD gives an excellent description of existing data on elastic electron-proton/neutron cross-sections. Results of a simultaneous fit of the nucleon form factors $G_{M,E}^{p,n}$ to the cross-sections are given. Information is obtained about the QCD-scale parameter Λ_{QCD}, as well as on the range of applicability of perturbative QCD calculations. Constraints on the hadronic wavefunctions are also obtained.

One of the fundamental aims in physics is the understanding of the structure of the nucleon. Electromagnetic interaction gives us a unique tool for its investigation. Concerning the elastic electron–nucleon scattering the properties of the nucleon are hidden in the four structure functions $G_{E,M}^{p,n}(Q^2)$.

It is believed now that the theory of strong interaction is given by quantum chromodynamics (QCD).[1] Perturbative QCD can be applied to exclusive proceses at large momentum transfer.[2,3] One of the questions to be answered is down to which momentum transfer Q^2 perturbation theory can be applied, and in which range of momentum transfer we can still obtain valuable information by comparison with experiment. The answer to that question is still controversial.[4]

We know that at low momentum transfer $|Q^2| < 1$ GeV^2/c^2 the application of meson dynamics leads to a satisfactory description of hadronic form factors and interactions.[5] As long as one cannot handle reliably QCD at low momentum transfer we have to face the problem of synthesizing both pictures – meson-dynamics at low Q^2 – perturbative QCD at asymptotic Q^2. The problem arising here can be exemplified in the structure function of the rho-nucleon interaction. We know from a strong interaction coupling scheme[5] that the structure function of the tensor interaction, for example, follows at low Q^2 to a very good approximation a monopole. Extrapolating this information to high Q^2 would lead to an asymptotic behavior of Q^{-2}. Perturbative QCD tells us that this is completely off.[3] Here we expect a behavior of Q^{-6} (up to log-corrections). Similarly, of course, we go completely wrong by simply extrapolating perturbative QCD results to low Q^2. Obviously there is a dramatic change from low to high momentum transfer.

In the present note, we show that a semiphenomenological synthesis of both[6] – meson and quark dynamics – is able to give a satisfactory description of existing experimental information. In addition valuable information on high momentum quantities is obtained.

According to our knowledge of a physical photon we understand its effective interaction with the nucleon being composed of two pieces: (i) a direct interaction with the nucleon and (ii) a term involving vector mesons (Fig. 1). In the time-like region ($t > 0$), the meson contributions are of course dominant near the meson poles (origin of vector meson dominance[7] (VMD)). However for $t < 0$ where the intermediate mesons are far off-shell the direct contributions are not negligible (extended vector meson dominance[6] (EVMD)). We define the form factors of the vector–particle nucleon interaction in the usual way by:

$$\langle p' | J_\mu^\alpha | p \rangle = \frac{g_\alpha}{2}\, u(p') \left[F_1^\alpha(t)\gamma_\mu + \frac{i\sigma_{\mu\nu}(p'-p)^\nu}{2M}\kappa_\alpha F_2^\alpha(t) \right] \tau_3\, u(p) \qquad (1)$$

for isovector particles α and correspondingly for isoscalar ones (replace $\tau_3 \to 1$). $g_\alpha/2$ denotes the coupling of vector – particle – nucleon interaction at $t = 0$, κ_α is the ratio of tensor to vector coupling at $t = 0$. Throughout we consider space-like momentum transfer *i.e.*, $t = q^2 = (p'-p)^2 = -Q^2 < 0$.

Assuming a common vector and tensor form factor F_1 and F_2 respectively for all vector particles *i.e.*, $F_1 = F_1^\rho = F_1^\omega = F_1^\gamma$ and $F_2 = F_2^\rho = F_2^\omega = F_2^\gamma$, the e.m. nucleon form factors for a physical photon are given by extended vector meson dominance by:

$$\begin{aligned}
F_1^{IV}(Q^2) &= \left[\frac{m_\rho^2}{m_\rho^2+Q^2}\,\frac{g_\rho}{f_\rho} + \left(1 - \frac{g_\rho}{f_\rho}\right) \right] F_1(Q^2) \\
\kappa_V F_2^{IV}(Q^2) &= \left[\frac{m_\rho^2}{m_\rho^2+Q^2}\,\frac{\kappa_\rho g_\rho}{f_\rho} + \left(\kappa_V - \frac{\kappa_\rho g_\rho}{f_\rho}\right) \right] F_2(Q^2) \\
F_1^{IS}(Q^2) &= \left[\frac{m_\omega^2}{m_\omega^2+Q^2}\,\frac{g_\omega}{f_\omega} + \left(1 - \frac{g_\omega}{f_\omega}\right) \right] F_1(Q^2) \\
\kappa_S F_2^{IS}(Q^2) &= \left[\frac{m_\omega^2}{m_\omega^2+Q^2}\,\frac{\kappa_\omega g_\omega}{f_\omega} + \left(\kappa_S - \frac{\kappa_\omega g_\omega}{f_\omega}\right) \right] F_2(Q^2)
\end{aligned} \qquad (2)$$

with $\kappa_V = 3.706$, $\kappa_S = -.12$, $m_\rho = .776$ GeV, $m_\omega = .784$ GeV. m_α^2/f_α is the coupling of the photon to the vectormeson ($\alpha = \rho, \omega$).

In deriving Eq. (2) we considered a complete decoupling of the ϕ-meson from the nucleon *i.e.*, $g_\phi = 0$ according to the Zweig rule. This is not necessary but the experiment does actually favor this. Heavier vector mesons are not taken into account because of suppression of the coupling constants. It is actually not necessary to consider common form factors for isoscalar and isovector particle nucleon form factors. The comparison with the data, however, shows that they are very close and more precise data are necessary to distinguish between F_i^ω, F_i^ρ. Similarly, we used the simple expression for the meson propagators. Width effects do not show up to be important.

The electric and magnetic form factors G_E and G_M are given by:

$$G_M^p(Q^2) = F_1^p(Q^2) + F_2^p(Q^2) \quad ; \quad G_E^p(Q^2) = F_1^p(Q^2) - \frac{Q^2}{4M^2}\, F_2^p(Q^2) \quad , \qquad (3)$$

for the proton and accordingly for the neutron ($p \to n$).

The proton/neutron Dirac and Pauli form factors are:

$$\begin{aligned} F_1^p &= \frac{1}{2}\left(F_1^{IS} + F_1^{IV}\right) \quad ; \quad F_1^n = \frac{1}{2}\left(F_1^{IS} - F_1^{IV}\right) \\ F_2^p &= \frac{1}{2}\left(\kappa_S F_1^{IS} + \kappa_V F_2^{IV}\right) \quad ; \quad F_2^n = \frac{1}{2}\left(\kappa_S F_2^{IS} - \kappa_V F_2^{IV}\right). \end{aligned} \qquad (4)$$

Apart from the form factors F_1, F_2, Eq. (2) contains only low-energy quantities. The crucial connection between meson-dynamics and quark dynamics is therefore hidden in these functions. The low momentum ($Q^2 < 1$ GeV^2/c^2) dependence of F_1, F_2 is known from meson physics to be to a very good approximation of monopole type:[5]

low Q^2

$$F_1 \sim F_2 \sim \frac{\Lambda_1^2}{\Lambda_1^2 + Q^2} \text{ with } \Lambda_1 \sim 0.8 \text{ GeV} . \qquad (5)$$

The high Q^2 behavior for nucleons can be calculated in perturbative QCD:[3]

large Q^2

$$F_1 \sim \left[\frac{1}{Q^2 \log\left(Q^2/\Lambda^2_{QCD}\right)}\right]^2$$
$$F_2 \sim \frac{F_1}{Q^2} \tag{6}$$

For the interpolation between low and high Q^2 it is convenient to use a simple form:

$$F_1(Q^2) = \frac{\Lambda_1^2}{\Lambda_1^2 + \hat{Q}^2} \cdot \frac{\Lambda_2^2}{\Lambda_2^2 + \hat{Q}^2}$$
$$F_2(Q^2) = \frac{\Lambda_1^2}{\Lambda_1^2 + \hat{Q}^2} \cdot \left[\frac{\Lambda_2^2}{\Lambda_2^2 + \hat{Q}^2}\right]^2 \tag{7}$$

with

$$\hat{Q}^2 = Q^2 \log\left(\frac{\Lambda_2^2 + Q^2}{\Lambda^2_{QCD}}\right) \Big/ \log\left(\frac{\Lambda_2^2}{\Lambda^2_{QCD}}\right)$$

For $\Lambda_2^2 \gg \Lambda_1^2$ we realize that we recover the low-momentum behavior for the functions F_1, F_2, as well as the high Q^2 behavior as predicted by QCD.

In order to understand the role of Λ_2, Λ_{QCD} it is instructive to consider the different limits in more detail:

$Q^2 \ll \Lambda_2^2$: F_1, F_2 are completely dominated by meson dynamics. F_1, F_2 $\rightarrow$ monopole.

$Q^2 \gg \Lambda_2^2$: F_1, F_2 are completely dominated by quark dynamics.

: F_1, F_2 follow the asymptotic QCD predictions.

: $F_1 \rightarrow \Lambda_1^2\Lambda_2^2/\hat{Q}^4$, $F_2 \rightarrow \Lambda_1^2\Lambda_2^4/\hat{Q}^6$

Comparison of the value $\Lambda_1^2\Lambda_2^2$ with experiment will give us information on the quark wavefunction of the nucleon.

$Q^2 \sim \Lambda_2^2$: Around this momentum transfer both – meson and quark dynamics – will be important.

Due to the additional power suppression of Q^2 in the meson propagator the meson terms die out rather fast as Q^2 increases and we are left with the direct photon nucleon coupling terms which gives the correct asymptotics for the e.m. nucleon form factors. Note that apart from the quantities Λ_2 and Λ_{QCD} which determine the medium and high momentum behavior of the electric and magnetic nucleon form factors, we have only low energy quantities involved, most of which are known. For example, $SU(3)_F$ determines $g_\rho/g_\omega = \sin\theta/\sqrt{3}$, $g_\phi = 0$ for θ near ideal mixing angle, κ_ρ and κ_ω are known from pion–nucleon scattering: $\kappa_\rho = 6.1 \pm .6$[8] and $\kappa_\omega = .14 \pm .2$[9], $\Lambda_1 \sim 0.8$ GeV from a strong interaction coupling scheme.[5]

Instead of taking the information we have on the different low energy quantities we determine them by a fit procedure and compare afterwards. We performed a complete analysis of the elastic electron scattering data by a simultaneous fit of all four form factors $G_{M,E}^{p,n}$ to the available cross-sections.

As far as proton data are concerned we use the data analyzed in Refs. 10 – 12 up to $Q^2 \sim 5\text{GeV}^2/c^2$. As for high momentum data we use the Stanford data[13] with the normalization determined according to the low momentum analysis.[10–12] Neutron cross-sections are taken from Refs. 14, 15.

The best fit parameters determining the functions F_i^{IS}, F_i^{IV} Eqs. (2) and (7) are summarized in Table 1 together with the information from other sources (in parenthesis). We note an overall agreement of the best fit parameters with the known values, which gives some credibility to the obtained values of $\Lambda_2 = 2.27$ GeV and $\Lambda_{QCD} = .29$ GeV. Actually we could have fixed most of the fit quantities by using the known information. Note that our analysis shows a decoupling of the ϕ–meson from the nucleon according to the Zweig rule,[19] and no higher mesons are necessary in contrast to the conventional vector meson dominance models.[20]

The resulting functions $G_{M,P}$, using the best fit values of Table 1 are shown in Figs. 2 – 5 in a $Q^4 G_{M,P}$ plot, which emphasizes the high momentum behavior. We do not show a comparison at low momentum in this note, however, the

description of the low momentum data is excellent as indicates by $\chi^2_{\rm tot}/N = .43$ (see also Table 2).

The proton magnetic form factor is shown in Fig. 2. In addition to the total form factor we also show the contributions arising from proton Dirac (F_1^p)– and proton Pauli (F_2^p)–form factor. We see that at high momentum transfer G_M^p is dominated by F_1^p. This is expected from QCD scaling as for $Q^2 \to \infty$ we have $F_1^p/F_2^p \sim Q^2$. The more recent, unpublished, Stanford data[21] lie somewhat higher. Adjustment to these data would imply $\Lambda_{QCD} \sim 0.2$ GeV. (But this might be a normalization problem which we did not investigate.) The data above $Q^2 \sim 20$ GeV$^2/c^2$ cannot be explained. It is interesting to see the effect of a variation in Λ_{QCD}. Neglecting the log-dependence in G_M^p it i.e., $\hat{Q}^2 = Q^2$ in Eq. (7), we obtain the curve labeled $\Lambda_{QCD} = 0$. The present data limit Λ_{QCD} (in our parametrization) to the range of 0.2 - 0.5 GeV. More precise data can put limits on Λ_{QCD}, Λ_2 which are closer.

The electric proton form factor G_E^p is shown in Fig. 3. Here we have a completely different situation. Instead of the sum of F_1^p and F_2^p we have $G_E^p = F_1^p - (Q^2/4M^2)F_2^p$ indicating that both F_1^p and F_2^p are important at high Q^2, in contrast to the case of G_M^p. This results in a strong cancellation. Note that the difference of two large numbers is very uncertain. Unfortunately high precision data[11] are available only in the range up to a $Q^2 \lesssim 1.5$GeV$^2/c^2$. Although our G_E^p describes the data very well ($\chi^2/N = .44$) up to this momentum transfer, the form factor above $Q^2 = 2$GeV$^2/c^2$ is very uncertain because of this delicate cancellation. Small changes in the coupling constants can largely enhance or reduce G_E^p. Precise measurements of G_E^p at high Q^2 would therefore be highly desirable.

Figures 4, 5 show the neutron form factors G_M^n and G_E^n together with the data of Albrecht *et al.*,[14] and S. Rock *et al.*[15] Before comparing with the data it is interesting to have a close look at the neutron Dirac form factor F_1^n. According to the definition, Eq. (4), and the fact that $m_\rho \sim m_\omega$ and $g_\rho/f_\rho \sim g_\omega/f_\omega$, we

find $F_1^n = F_1^{IS} - F_1^{IV} \sim 0$.

This finding is independent of the vector particle nucleon form factor and thus independent of momentum transfer. As no such cancellation occurs in F_2^n due to the large difference between κ_V and κ_S, this means that both G_M^n and G_E^n are dominated at high Q^2 by F_2^n.

$$G_M^n \sim F_2^n \sim Q^{-6} \quad \text{and} \quad G_E^p \sim \frac{-Q^2}{4M^2} F_2^n \sim Q^{-4}$$

Thus G_M^n is effectively suppressed by a power of Q^2 as compared to G_M^p. In contrast G_E^n is larger than G_E^p at high Q^2.

This behavior is shown in Figs. 4, 5. Again we show the form factors with and without the log–corrections.

From the differences between proton and neutron form factors obtained in the present analysis we realize that we have to be careful in what quantities to compare with experiment. For example, the cross–section ratio of neutron to proton σ_n/σ_p decreases for high Q^2 solely because of the suppression of F_1^n. This shows that one cannot look only for scaling properties in the comparison with experiment. On the other hand, however, the asymptotic strengths of the functions F_i, $F_i^{IV,IS}$ as determined by experiment will give us severe constraints on the hadronic quark wavefunctions. As far as the quantities Λ_2, Λ_{QCD} in this analysis are concerned we note that although the present data prefer $\Lambda_2 = 2.27$ GeV and $\Lambda_{QCD} = .29$ GeV (using our parametrizations) the data at high momentum transfer are not accurate enough to exclude somewhat larger values. The fact that Λ_2/Λ_{QCD} is large is to be connected with the relevant scales which control QCD. The present finding might have some consequences on the conclusions reached in Ref. 4, the hadron phenomenology of Ref. 22 as well as on the size of the core of the bag models.

One of us (M.G.) is grateful to S. J. Brodsky for a discussion on the manuscript.

REFERENCES

1. Reviews of QCD: A. J. Buras, Rev. Mod. Phys. 53, 199 (1980); A. H. Mueller, Phys. Rep. 73C, 237 (1981); E. Reya, Phys. Rep. 69, 195, (1981).

2. G. R. Farrar and D. R. Jackson, Phys. Rev. Lett. 43, 246 (1979); A. V. Efremov and A. V. Radyushkin, Phys. Lett. 94B, 245 (1980); A. Duncan and A. H. Mueller, Phys. Lett. 90B, 159 (1980); Phys. Rev. D21, 1626 (1980).

3. S. J. Brodsky and G. Farrar, Phys. Rev. D11, 1309 (1975); S. J. Brodsky and G. P. Lepage, Phys. Scr. 23, 945 (1981); G. P. Lepage and S. J. Brodsky, Phys. Rev. D22, 2157 (1980).

4. N. Isgur and C. H. Llewellyn Smith, Phys. Rev. Lett. 52, 1080 (1984).

5. U. Kaulfuβ and M. Gari, Nucl. Phys. A408, 507 (1983); M. Gari and U. Kaulfuβ, Phys. Lett. 136B, 139 (1984).

6. M. Gari and W. Krümpelmann, Phys. Lett. 141B, 295 (1984).

7. For a summary see J. J. Sakurai in: Currents and Mesons (University of Chicago Press).

8. G. Höhler and E. Pietarinen, Nucl. Phys. B95, 210 (1975) and Nucl. Phys. B216, 334 (1983).

9. W. Grein and P. Kroll, Nucl. Phys. A338, 332 (1980).

10. G. Höhler, *et al.,* Nucl. Phys. B114, 505 (1976).

11. F. Borkowski, *et al.,* Z. Phys. A275, 29 (1975); Nucl. Phys. B93, 461 (1975).

12. G. G. Simon, *et al.,* Z. Naturforsch. 35a, 1 – 8 (1980).

13. P. N. Kirk, *et al.,* Phys. Rev. D8, 63 (1973).

14. W. Albrecht, *et al.,* Phys. Lett. 26B, 642 (1968).

15. S. Rock, *et al.,* Phys. Rev. Lett. 49, 1139 (1982).

16. Yu. K. Akimov, *et al.* as quoted in F. Iachello *et al.,* Phys. Lett. 43B, 191 (1973).

17. V. E. Krohn and G. R. Ringo, Phys. Rev. 148, 1303 (1966).

18. L. Koester, *et al.,* Phys. Rev. Lett. 36, 1021 (1976).

19. J. Mandula, *et al.,* Ann. Rev. Nucl. Sci. 20, 289 (1970).

20. H. Genz and G. Höhler, Phys. Lett. 61B, 389 (1976).

21. W. B. Atwood, Ph.D. thesis Stanford University, SLAC Report No. 185, (1975) (unpublished); M. D. Mestayer, Ph.D. thesis, Stanford University SLAC Report No. 214, (1978) (unpublished).

22. S. J. Brodsky, T. Huang and G. P. Lepage, Particles and Fields 2, 143 (1983), edited by A. Z. Capri and A. N. Kamal (Plenum Publishing Company).

Table 1

Parameters determined by a simultaneous fit to the avaliable cross-sections. The values given in parenthesis are from other experiments or $SU(3)$, see text.

					[GeV]		
χ^2_{tot}/N	g_ρ/f_ρ	κ_ρ	g_ω/f_ω	κ_ω	Λ_1	Λ_2	Λ_{QCD}
.43	.377	6.62	.411	.163	.795	2.27	.29
		$(6.1 \pm .6)$	$(\sim .4)$	$(.14 \pm .2)$	$(\sim .8)$		

Table 2

Calculated slopes for $G_E^p(t)$ and $G_E^n(t)$ in comparison with experimental data.

	$[\mathrm{GeV/c}]^{-2}$	
	$dG_E^p/dt\|_{t=0}$	$dG_E^n/dt\|_{t=0}$
best fit	-2.92	.52
experiment	$-2.92 \pm .11$ [16]	$.52 \pm .007$ [18]
		$.496 \pm .010$ [17]

Figure Captions

Figure 1 Illustration of extended vector meson dominance (EVMD): a) physical photon propagator b) coupling of a physical photon to the nucleon.

Figure 2 Proton magnetic form factor $G_M^p(Q^2)$. The data points are from the analysis in Refs. 10 - 12 and our analysis of the cross sections of Ref. 13.

Figure 3 Proton electric form factor $G_E^p(Q^2)$. $(\tau = Q^2/4M^2)$. Data points are from Refs. 10 - 12.

Figure 4 Neutron magnetic form factor $G_M^n(Q^2)$. Data points are from our analysis of the cross sections in Ref. (14) ($\circ$) and Ref. 15 ($\bullet$).

Figure 5 Neutron electric form factor $G_E^n(Q^2)$. $(\tau = Q^2/4M^2)$. Data points are from our analysis of the cross sections in Ref. 14 ($\circ$) and Ref. 15 ($\bullet$).

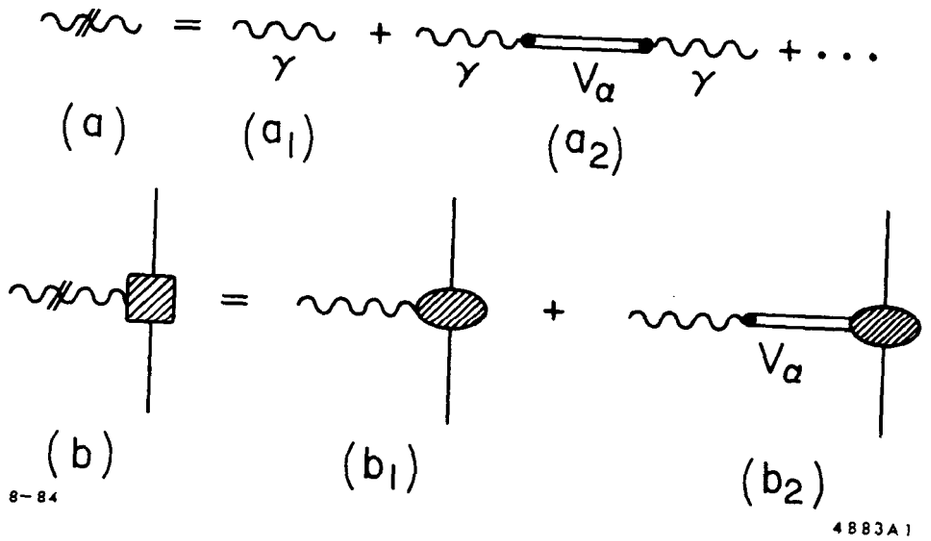

Fig. 1

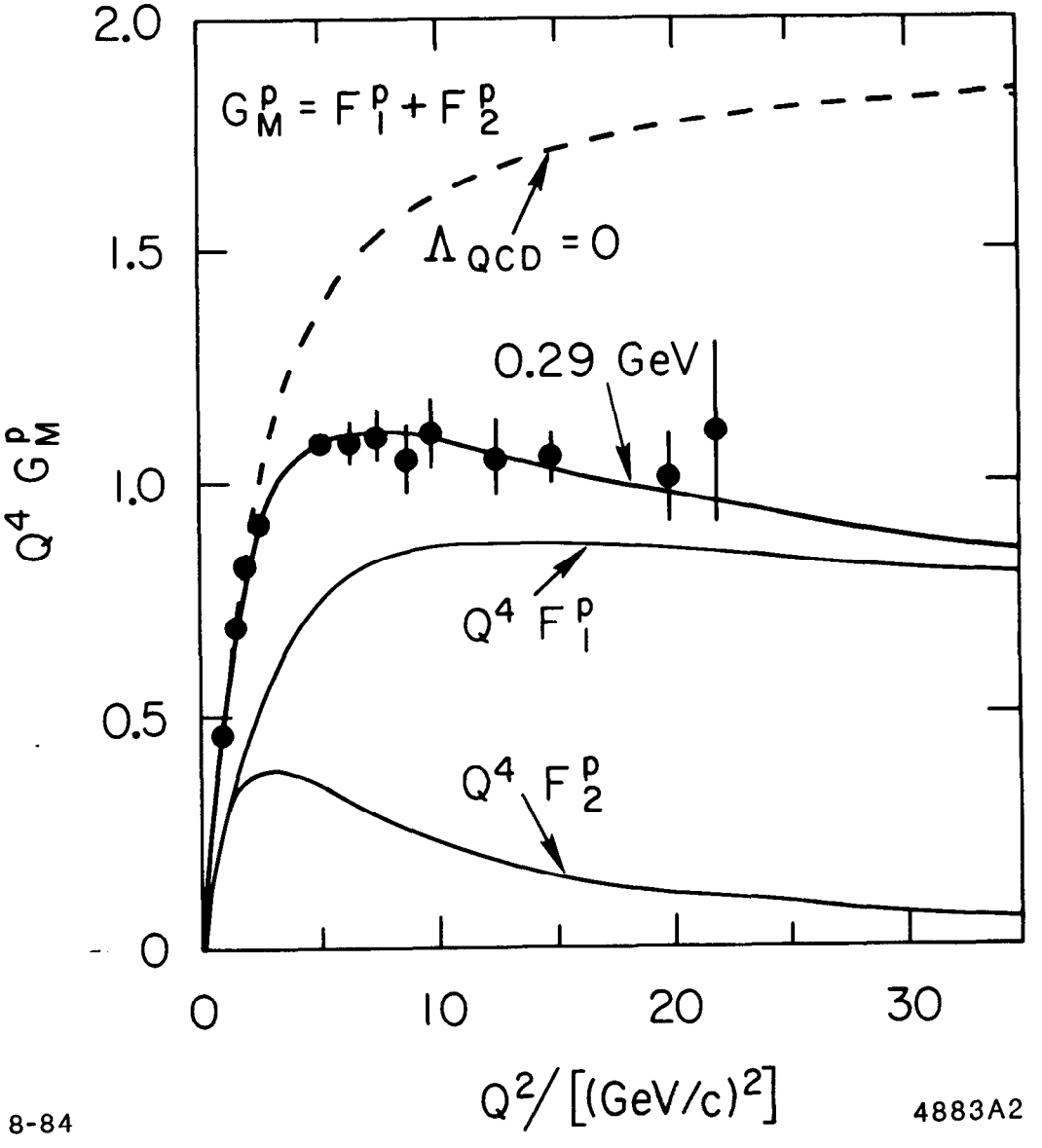
2.0
1.5
1.0
0.5
0
$G_M^p = F_1^p + F_2^p$
$\Lambda_{QCD} = 0$
0.29 GeV
$Q^4 F_1^p$
$Q^4 F_2^p$
$Q^4 G_M^p$
0
10
20
30
$Q^2/[(GeV/c)^2]$
8-84
4883A2

Fig. 2

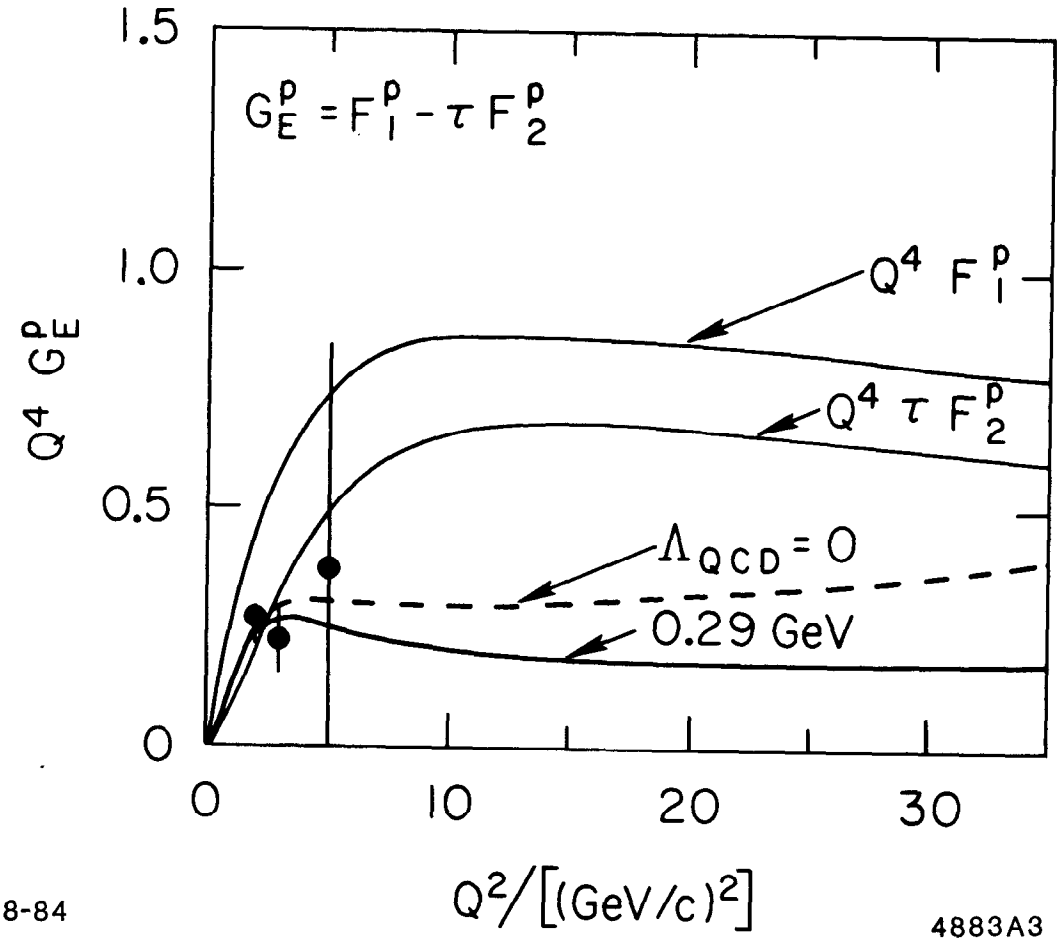
1.5
1.0
0.5
0
$G_E^p = F_1^p - \tau F_2^p$
$Q^4 F_1^p$
$Q^4 \tau F_2^p$
$\Lambda_{QCD} = 0$
0.29 GeV
$Q^4 G_E^p$
0
10
20
30
$Q^2/[(GeV/c)^2]$
8-84
4883A3

Fig. 3

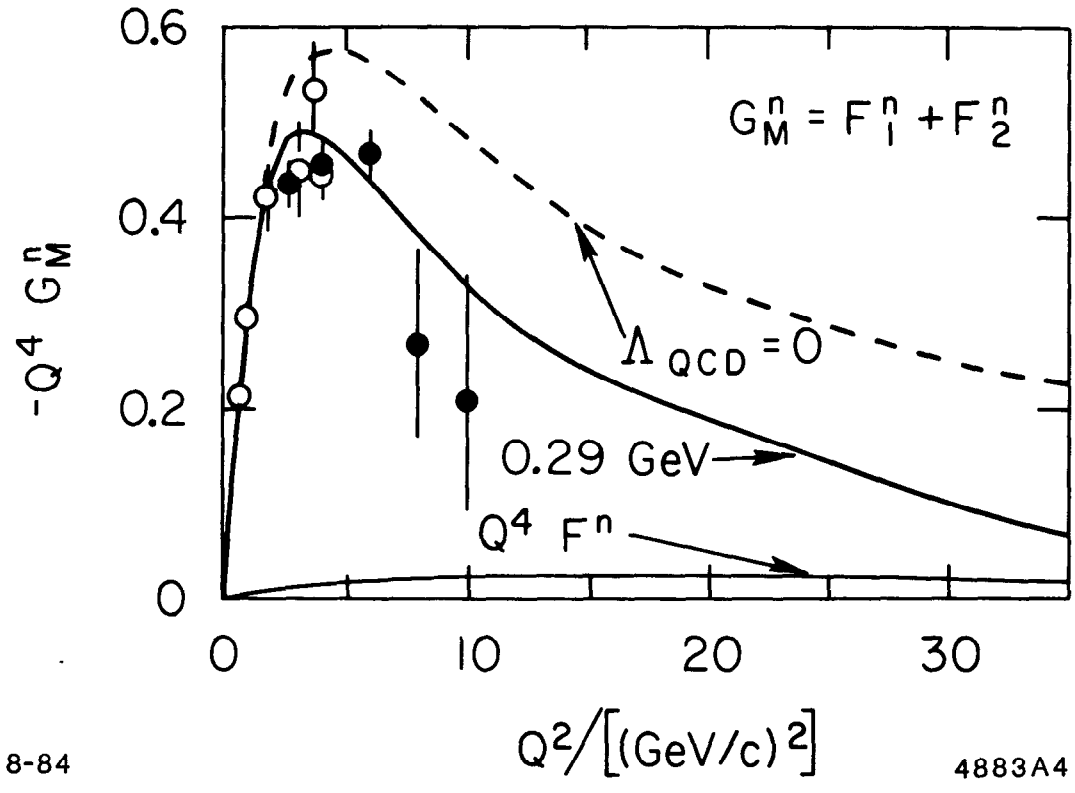
0.6
0.4
0.2
0
$-Q^4 G_M^n$
$G_M^n = F_1^n + F_2^n$
$\Lambda_{QCD} = 0$
0.29 GeV
$Q^4 F^n$
0
10
20
30
$Q^2/[(GeV/c)^2]$
8-84
4883A4

Fig. 4

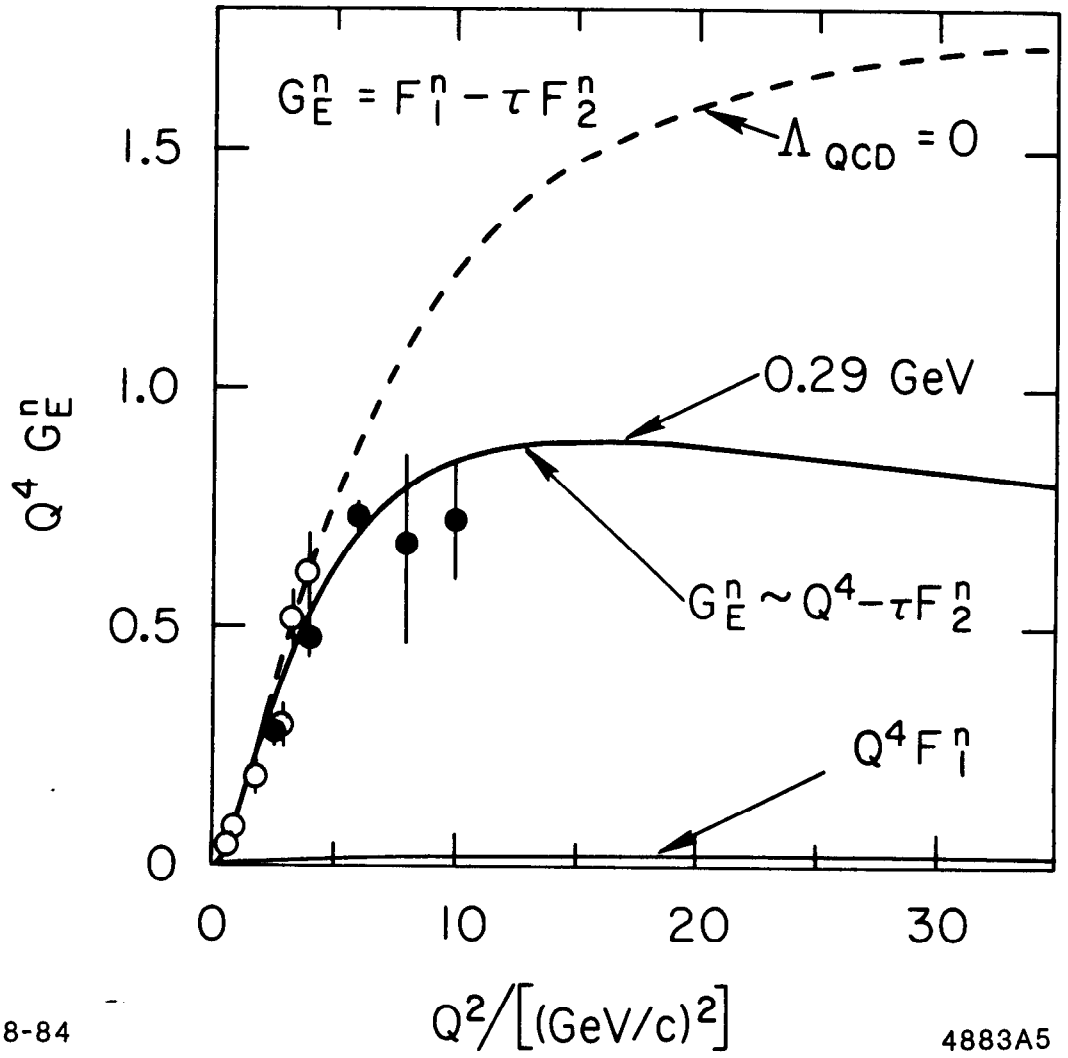
$G_E^n = F_1^n - \tau F_2^n$
$\Lambda_{QCD} = 0$
0.29 GeV
$G_E^n \sim Q^4 - \tau F_2^n$
$Q^4 F_1^n$
$Q^4 G_E^n$
1.5
1.0
0.5
0
0
10
20
30
$Q^2/[(GeV/c)^2]$
8-84
4883A5

Fig. 5